Recent density functional studies of hydrodesulfurization catalysts: insight into structure and mechanism

2008 J. Phys.: Condens. Matter 20 064236

(http://iopscience.iop.org/0953-8984/20/6/064236)

IOP Publishing Journal of Physics: Condensed Matter

J. Phys.: Condens. Matter **20** (2008) 064236 (8pp) doi:10.1088/0953-8984/20/6/064236

Recent density functional studies of hydrodesulfurization catalysts: insight into structure and mechanism

Berit Hinnemann[1], **Poul Georg Moses**[2] **and Jens K Nørskov**[2]

[1] Haldor Topsøe A/S, Nymøllevej 55, DK-2800 Lyngby, Denmark
[2] Department of Physics and Center for Atomic-scale Materials Design (CAMD), NanoDTU, Technical University of Denmark, DK-2800 Lyngby, Denmark

E-mail: behi@topsoe.dk

Received 17 September 2007, in final form 29 November 2007
Published 24 January 2008
Online at stacks.iop.org/JPhysCM/20/064236

Abstract

The present article will highlight some recent density functional theory (DFT) studies of hydrodesulfurization (HDS) catalysts. It will be summarized how DFT in combination with experimental studies can give a detailed picture of the structure of the active phase. Furthermore, we have used DFT to investigate the reaction pathway for thiophene HDS, and we find that the reaction entails a complex interplay of different active sites, depending on reaction conditions. An investigation of pyridine inhibition confirmed some of these results. These fundamental insights constitute a basis for rational improvement of HDS catalysts, as they have provided important structure–activity relationships.

(Some figures in this article are in colour only in the electronic version)

1. Introduction

While the global energy consumption is steadily increasing, fossil energy resources become increasingly limited. This increases the need to upgrade low-quality oil to transport fuels. At the same time, environmental restrictions become stricter. One key environmental requirement is the reduction of sulfur content in the fuel. This necessitates substantial improvements of the hydrodesulfurization (HDS) catalysts, which remove sulfur-containing compounds from crude oil during the refining process [1–9]. In particular, these catalysts must now be able to remove sulfur from compounds where it is both strongly bound within an organic ring compound and possibly also sterically protected, e.g. in methylated dibenzothiophenes (DBTs).

For rational improvements of the HDS catalyst, a detailed understanding of its structure and reactivity is necessary, and this is a formidable challenge given the complexity of the catalyst over several length scales. HDS catalysts commonly consist of Co- and/or Ni-promoted MoS_2 nanostructures as active phase on a high-surface area porous support, typically γ-alumina. A complete description of this complicated system is demanding. Detailed understanding of the active phase structure under reaction conditions is required, and issues like active phase–support interactions and active phase dispersion need to be addressed. A detailed characterization and understanding of catalyst activity and reaction mechanism is complicated by the fact that a typical feedstock contains numerous sulfur-containing compounds, whose reaction mechanisms for HDS may differ. Also, inhibition of HDS by nitrogen-containing compounds, e.g. pyridine, needs to be considered, and often these compounds are first removed from the feedstock by hydrodenitrogenation (HDN).

Even though HDS catalysts have been investigated with different experimental techniques for numerous years [1], not much information about the structure of the active phase under catalytic turnover was available until the 1980s. About that time, a combination of several experimental techniques like Mössbauer spectroscopy, extended x-ray absorption fine structure (EXAFS) and infrared (IR) spectroscopy evidenced a Co–Mo–S active phase, where Co (or Ni) is incorporated into small MoS_2-like nanosized crystals [10–14]. These are present as single or stacked layers on the catalyst support. Since the development of this 'Co–Mo–S' model, numerous experimental studies have refined the structure of the active phase. In particular, scanning tunnelling microscopy (STM) has provided the first atomic-scale resolved information on the structure of unpromoted and promoted MoS_2 nanoparticles [15–17]. Recently, also high angle annular dark field scanning

transmission electron microscopy (HAADF-STEM) has given detailed structural information [18–20].

Despite all available studies, the understanding of HDS structure and reactivity and especially the development of structure–activity relationships remains a challenge. To this end, the advent of density functional theory (DFT) [21, 22] and the development of stable and precise calculational methods and software packages, such as VASP [23, 24], CASTEP [25, 26], DMol^3 [26, 27], Dacapo [28, 29], Abinit [30, 31], Wien2k [32, 33] and numerous other codes [34], provide unprecedented new opportunities for investigating the active phase structure and activity of HDS catalysts in atomic detail. Furthermore, the rapid growth of computational power allows investigation of larger and increasingly realistic model systems. First-principles techniques like DFT allow for investigation of active sites and reaction pathways on an atomic scale, and in this way they have improved our understanding of the HDS process. A particular strength of DFT and related modelling is that it enables probing of specific aspects and questions, which are often not as easily singled out in an experiment.

In this review, we will provide an overview on our DFT activities within HDS catalysis during recent years. We will start by reviewing our work on elucidating both the atomic and the electronic structure of the active phase in detail, where a combination of scanning tunnelling microscopy and density functional theory has proven very successful. We note that a number of groups have contributed significantly to the present theoretical description of the HDS reaction [35–80]. We will also give a short discussion of support effects. Finally, we will summarize our DFT efforts in understanding the HDS of thiophene and its inhibition by pyridine in atomic-scale detail. Our results suggest several activity descriptors that may be useful for designing better HDS catalysts. We will conclude the paper with a discussion on how DFT, most often in combination with experimental techniques, helps us to understand HDS catalysis.

All DFT results which are presented here have been obtained using the DFT code Dacapo [28, 29], which uses plane waves as a basis set and therefore is ideal for the study of periodic systems. The ion–electron interactions are treated by Vanderbilt ultrasoft pseudopotentials [81]. The exchange–correlation energy is included by the generalized gradient approximation (GGA) using the PW91 exchange–correlation functional [82]. From the electronic structure, it is possible to generate simulated STM images, and we have used the Tersoff–Hamann model [83] to do this. The nudged elastic band (NEB) method [84] allows for an efficient calculation of saddle points and reaction pathways.

2. Structure of MoS_2, Co–Mo–S and Ni–Mo–S

A prerequisite for HDS activity studies using theoretical models is detailed structural information about the active phase under reaction conditions. Even though the industrial catalyst consists of Co- or Ni-promoted MoS_2, it is instructive to understand the unpromoted MoS_2 phase first. As shown in figure 1, MoS_2 consists of layered hexagonal sheets as S–Mo–S

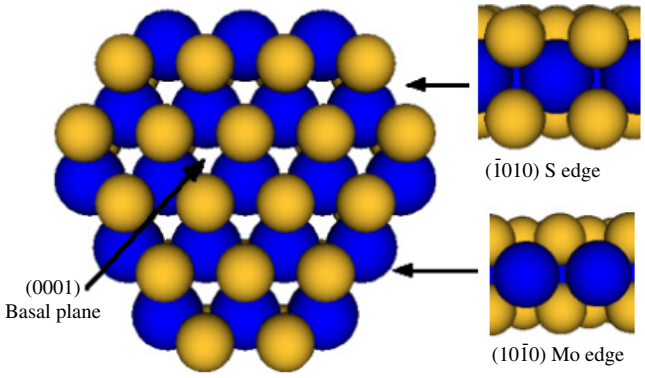

Figure 1. Structure of MoS_2 and the two low-index edge terminations. Colour code: molybdenum, dark (blue online); sulfur, light (yellow online). Note that the edge terminations are shown as truncated from the bulk, not as they are present in a specific gaseous environment.

sandwiches. In the pure compounds the sheets are stacked and held together by van der Waals forces so that MoS_2 in some aspects resembles graphite. A sheet has two low-index edge terminations, the (10$\bar{1}$0) Mo edge and the ($\bar{1}$010) S edge. It is well known from numerous experimental studies [1] that the basal plane of MoS_2 is inert and that only the edges exhibit catalytic activity. Thus, it is of fundamental importance to elucidate the detailed edge structure under catalytic conditions, as changing the termination and structure of the exposed edges by e.g. the addition of Co and Ni promoter atoms is one way to enhance catalyst activity.

The shape of the nanoparticle depends on the relative edge free energies according to the Wulff construction, and this determines which edges will be exposed. Furthermore, under reaction conditions, where both H_2 and H_2S are present, the edges may have sulfur, hydrogen or SH groups adsorbed, and this in turn changes the edge free energies. DFT calculations as such provide total energies for structures at $T = 0$ K and in vacuum. To calculate free energies for non-zero temperatures and in the presence of a gas of a certain pressure and composition, a grand canonical formalism including the chemical potential of hydrogen and sulfur, which in turn depend on temperature and H_2 and H_2S partial pressures, has to be employed [43, 47, 57]. This scheme has also been applied to surface thermochemistry under oxidation (see e.g. [85]) and numerous other reactions, and can be regarded as a standard method to account for a finite temperature and the presence of a reactive gas.

An important step in elucidating the structure of unpromoted MoS_2 was the investigation of a model system, where MoS_2 was deposited on Au(111) by STM [15]. The STM images, taken under sulfiding conditions, showed that the MoS_2 was present as single-layer triangular nanoparticles, i.e. only one type of edge was exposed. Subsequently, DFT was used to calculate edge free energies for both the Mo edge and the S edge with a variety of configurations, and it could be concluded that under the STM conditions the (10$\bar{1}$0) Mo edge with adsorbed sulfur dimers is exposed [49], in line with theoretical studies by other research groups [43, 50, 60, 61, 75].

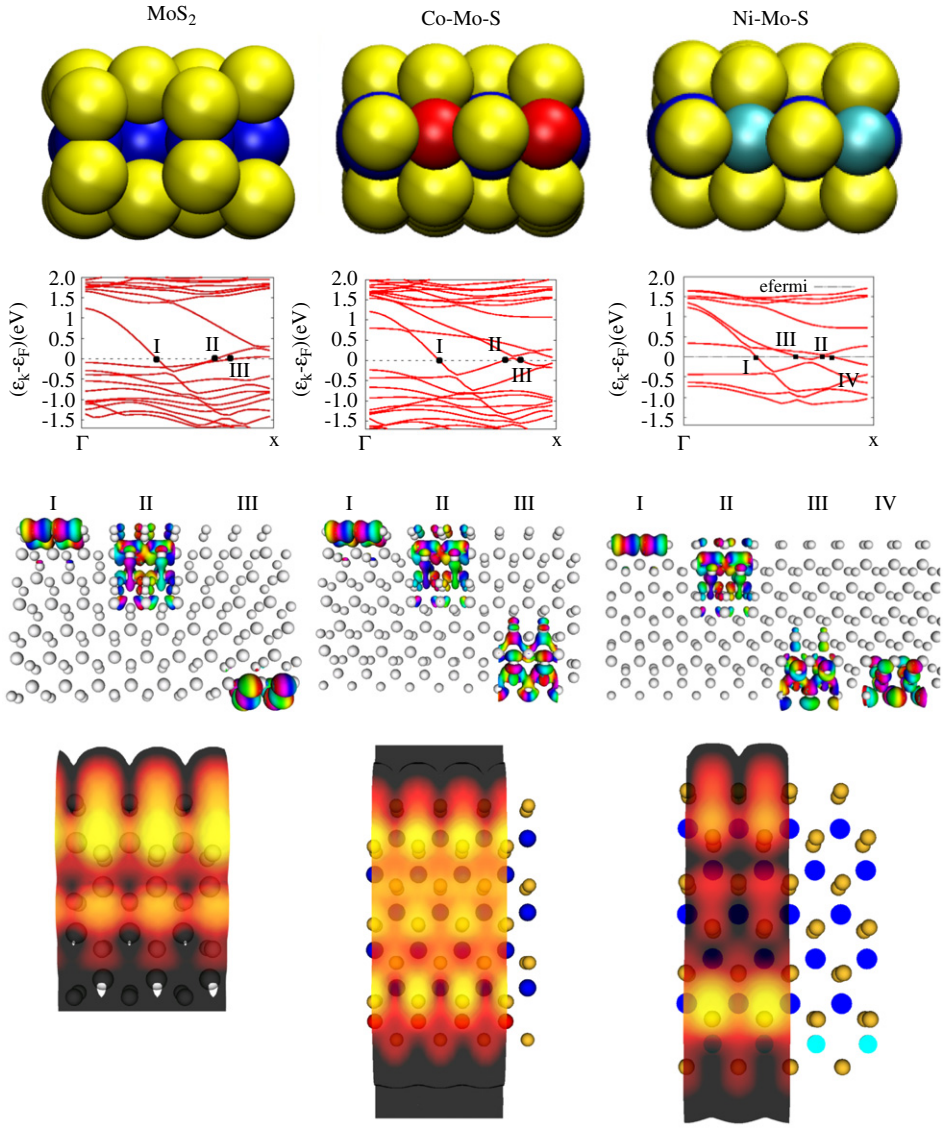

Figure 2. Calculated DFT edge structures, band structures, contour plots for the edge Kohn–Sham wavefunctions and STM simulations for MoS_2, Co–Mo–S and Ni–Mo–S structures. In the case of MoS_2 the Mo edge with sulfur dimers is shown; in the case of Co–Mo–S and Ni–Mo–S the promoted S edges with sulfur monomers are shown. For the STM plots note that for MoS_2 only the simulation for the Mo edge is depicted, whereas for Co–Mo–S and Ni–Mo–S structures the entire slab is shown. Colour code: molybdenum, blue; cobalt, red; nickel, light blue; sulfur, yellow (colours only available in the web version). Adapted from [17, 49, 57].

This edge configuration and the simulated STM image are shown in figure 2, and one can see that the protrusions in the simulated STM image actually are located between the S dimers and form a bright brim along the edge [49]. This bright brim could be understood by a detailed analysis of the electronic state at the Mo edge, and the band-structure diagram and contour plots of the relevant Kohn–Sham wavefunctions are depicted in figure 2. Bulk MoS_2 consisting of infinite sheets of S–Mo–S is semiconducting with a bandgap of about 1.2 eV [86], but the creation of edges, in this case the $(10\bar{1}0)$ Mo edge, creates electronic states around the Fermi level which have metallic character. Visualization of the Kohn–Sham wavefunction corresponding to these metallic states (figure 2) shows that they are one dimensional and localized at the edge. It should be mentioned that DFT calculations on both Au-supported and unsupported MoS_2 structures were performed, and that the metallic edge states were present in both systems and only slightly influenced by the presence of the Au support [49, 57].

It should be emphasized that a change in conditions, i.e. temperature and composition of the gas phase, especially H_2S/H_2 ratio, changes the extent to which the $(10\bar{1}0)$ Mo edge and the $(\bar{1}010)$ S edge are exposed and their respective sulfur and hydrogen coverage. Phase diagrams for edge structures over a range of temperatures and partial pressures of H_2 and H_2S have been constructed by several research groups [43, 50, 56, 57, 60, 61, 75] and it has also been shown using STM that the triangular MoS_2 particles assume hexagonal shape and their edge termination changes upon changing the gaseous atmosphere from sulfiding to reducing conditions [87].

Considering that the active phase of industrial catalysts is Co- and Ni-promoted MoS_2, it is most important to extend the detailed structural understanding to these promoted structures. According to the now well accepted Co–Mo–S model for the promoted MoS_2 hydrotreating catalysts, the Co and Ni promoter atoms are located at edge positions of MoS_2 nanostructures, which are believed to enhance catalytic activity by changing vacancy formation energies and the type and structure of the exposed edges. For the promoted structures, the approach of combining DFT with STM studies again has proven to be very insightful, and the resulting edge terminations, their simulated STM images and their electronic structure are shown in figure 2.

In the case of Co, the Co–Mo–S nanoparticles assume a hexagonal structure and expose both the $(10\bar{1}0)$ Mo edge and a Co-promoted $(\bar{1}010)$ S edge, in which Co substitutes a complete row of Mo atoms [16]. As the Mo edge remained unchanged upon the inclusion of Co, whereas the newly exposed S edge differs in appearance from the unpromoted S edge, it could be concluded that Co exclusively substituted at the S edge [17]. This assignment was in agreement with theoretical studies by other researchers [44, 51, 60, 75]. Thus, the substitution of Mo atoms by Co at the S edge changes the edge free energy such that the Co-promoted S edge is also exposed under sulfiding conditions. From the structure of the Co-promoted $(\bar{1}010)$ S edge (figure 2), one can see that the Co atoms prefer to be tetragonally coordinated to sulfur monomers.

Recently, calculations in the case of Ni-promoted MoS_2 were performed and also compared to STM images [17]. The STM images showed [17] that the case of Ni is much more complicated, as the position of the Ni seems to depend on the particle size. For large particles, Ni seems to change the MoS_2 in a similar way to Co, namely that it substitutes the outermost Mo atoms at the S edge. This results in a Ni-promoted S edge whose structure is shown in figure 2 and in which Ni is tetrahedrally coordinated to sulfur. For smaller Ni–Mo–S particles, however, Ni atoms substitute both at the Mo edge and the S edge, and it was found that higher-index edges are also exposed [17]. In particular, for Ni substitution at the metal edge, the most stable structure has Ni in a square-planar environment without any additional sulfur atoms bound to the edge, as also found previously [51, 60] and as one might expect from inorganic chemistry. In contrast to Co promotion, Ni does not seem to exhibit a clear preference for one edge over the other, and thus it can be located at one or both edges, depending on particle size. In addition, Ni was observed to cause exposure of higher-index edges [17], which is surprising considering that such edges were regarded to be too high in edge energy to be created.

Also the Co–Mo–S and Ni–Mo–S structures exhibit metallic edge states, as can be seen from their band structures and the corresponding Kohn–Sham wavefunctions depicted in figure 2. This is especially interesting in view of the fact that these metallic edge states exhibit catalytic activity for e.g. adsorption and hydrogenation of thiophene, as shown both experimentally and theoretically [88, 89]. A well established view on catalytic HDS activity is that activity mainly depends on the ability of the relevant edge structure to form vacancies, where sulfur-containing structures can adsorb and where sulfur can be removed. However, several recent studies have suggested that the brim sites also have catalytic activity under certain conditions [70, 76, 88, 89]. These aspects will be discussed in detail in section 3.

In conclusion, the combination of DFT with STM investigations and other experimental techniques has proven very powerful to elucidate the atomic-scale structure of both unpromoted and promoted MoS_2. By providing information which is directly comparable to experiments, structural models can be confirmed or disproved, and thus a very detailed understanding of structure and location and influence of the promoter atoms could be obtained.

3. Support effects

One of the central questions in HDS catalysis is how the MoS_2 active phase interacts with the support, and the most widely used and relevant support in industrial catalysis is γ-Al_2O_3. Detailed modelling of the interaction of a MoS_2 nanoparticle with the γ-Al_2O_3 surface is a formidable task, both because of the large number of atoms required in a model and because the precise location of non-spinel sites in γ-Al_2O_3 is not completely known and is still under discussion [90–95]. Several theoretical studies of the support effect of γ-Al_2O_3 have been published [66, 78, 75]. Due to the industrial importance of the Co–Mo–S/γ-Al_2O_3 system, many experimental investigations using different techniques have been carried out, and it was found that the intrinsic activity of the catalyst strongly depends on the sulfidation temperature [1]. For lower sulfidation temperatures, the intrinsic activity is considerably smaller than for higher sulfidation temperatures, and it was suggested that the lower activity was caused by the presence of some Mo–O–Al linkages between the MoS_2 and the alumina support. This Co–Mo–S structure with Mo–O–Al linkages is termed type I Co–Mo–S and the more active Co–Mo–S structure without these linkages is termed type II. Upon increase of the sulfidation temperature, the Mo–O–Al linkages are broken and the more active type II structure is obtained. Interestingly, it was observed that the amount of Co influences the transition temperature, where type II instead of type I Co–Mo–S is formed, and it was found that by increasing the amount of Co in the system the transition temperature decreases [1]. Since these factors have implications for catalyst synthesis and activity optimization, it was of particular interest to understand these trends within an atomistic model.

In a recent study [96], we have taken a very simple approach to study the influence of Mo–O–Al linkages on a MoS_2 catalyst and model the Mo–O–Al linkages by Mo–O–H groups. In this study we were mainly interested in the chemical and electronic consequences of these linkages and did not consider structural effects such as lattice mismatch or rigidity which are not included in this model.

The first question we wanted to answer was at which edge the linkages are formed, and this was investigated by placing the linkages at either the Mo edge, the S edge or at positions

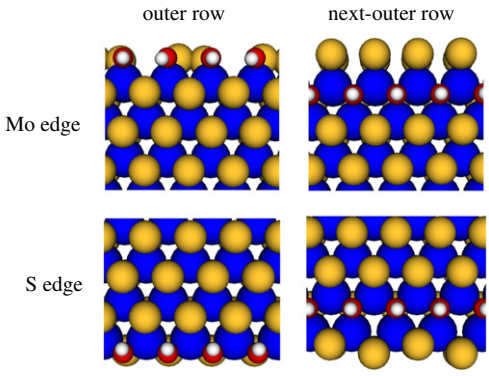

Position of OH group	linkages every row [kJ/mol]	linkages every sec. row [kJ/mol]
outer row at Mo edge	0	0
second row at Mo edge	89	25
second row at S edge	52	7
outer row at S edge	-152	-63

Figure 3. The investigated structures for the position of oxygen linkages and the corresponding energies (in kJ mol^{-1}) for the creation of linkages. Linkages at the outer row of the Mo edge are taken as the reference energy. Colour code: molybdenum, blue; sulfur, yellow; oxygen, red; hydrogen, white (colours only available in the web version). Adapted from [96].

in the next-outer rows, as shown in figure 3. Comparing the energies of the different structures, it could be concluded that the linkages will mostly form at the S edge, as they are energetically much more stable there. This result in itself is quite interesting, as it implies that the linkages are located at the same edge as Co promoter atoms are incorporated. This suggests that the more Co atoms are incorporated at the S edge, the fewer linkages are formed, and this is in accordance with the observation that the type I/type II transition temperature drops with increasing Co content. We also investigated the vacancy formation, as this is one indicator for catalytic activity, and found that it is energetically very expensive to form vacancies both at linkage sites and at the sites next to them. This effect could explain the reduced activity of type I Co–Mo–S structures, where linkages are present.

This very simple model for support linkages allowed us to understand some general trends concerning the reactivity of type I/type II catalyst. Even though the conclusions need validation using a more sophisticated model where the alumina support is included, our model proved useful in providing a framework in which to consider the effect of support linkages.

4. Reactivity and inhibition

A large number of experimental studies have investigated the kinetics of various HDS reactions and have provided insight into areas such as reaction networks, inhibition, and the influence of promoters [1, 8, 97, 98]. They made the general observation that there exist two different reaction pathways in HDS of cyclic sulfur-containing compounds. The first pathway, termed the hydrogenation pathway (HYD), is initiated by hydrogenation followed by S removal. In contrast, in the second pathway, which is termed the direct desulfurization (DDS) pathway, S is removed from the organic compound directly without prior hydrogenation. There is experimental evidence that the two pathways have different active sites [1], but so far it has not been established at which sites they take place.

It would be very relevant to elucidate the structure of the active site for hydrogenation and for desulfurization and to establish at which edges these reactions occur. The answers to these fundamental questions may have implications for catalyst design and synthesis, as it often is desirable to enhance specific properties, e.g. hydrogenation ability, of a catalyst. Knowing the nature of the active sites could provide guidance for optimizing the number of active sites. Furthermore, it would be valuable to know the elementary reaction steps that occur during HDS. Insight into the elementary reactions of HDS catalysis may also guide the development of catalysts with low hydrogen consumption and at the same time high HDS activity.

Density functional theory is well suited for answering questions about reactivity and structure and has done so for less complicated catalytic reactions, e.g. ammonia synthesis [99] or CO oxidation [85]. DFT studies on HDS by us [76, 88, 89] and other groups [36, 41, 59, 65, 75, 79] are also starting to provide detailed information on the elementary steps in the reaction pathway, and in this section some examples of how DFT has improved the insight into the reactivity of HDS catalysts are discussed.

Recently, we have performed a detailed DFT investigation of the HDS of thiophene over an unpromoted MoS_2 catalyst [76]. As a starting point for this study, it was very important to determine and use the edge structures as they are present under HDS conditions, and they differ from e.g. the edge structures under STM conditions, as discussed in the previous section. We used the phase diagrams developed previously [57], which describe the edge structure as a function of temperature and H_2 and H_2S partial pressures. It turned out that the active sites at the two edges are fundamentally different since the active site at the S edge is an undercoordinated vacancy site and the active site at the Mo edge is a so-called brim site (exhibiting a metallic edge state as discussed in the previous section), which is fully coordinated.

We then proceeded to calculate the elementary reaction barriers and intermediates for both the $(10\bar{1}0)$ Mo edge and the $(\bar{1}010)$ *S* edge. The calculations revealed that the hydrogenation steps in the HYD pathway should preferably take place at the Mo edge. However, all S–C bond scission steps, i.e. the final S–C scission step in the HYD pathway and S–C scission in the DDS pathway, seem to be more facile at the S edge, and therefore they probably take place there. The potential energy surface and intermediate structures for the HYD pathway and the DDS pathway on the S edge are shown in figure 4 and illustrate the complexity of this reaction. On a quantitative basis, these reaction pathways allow us to specify the contribution of each edge to the different reaction steps, and such investigations are in process. We emphasize that the discussed activity relations hold for

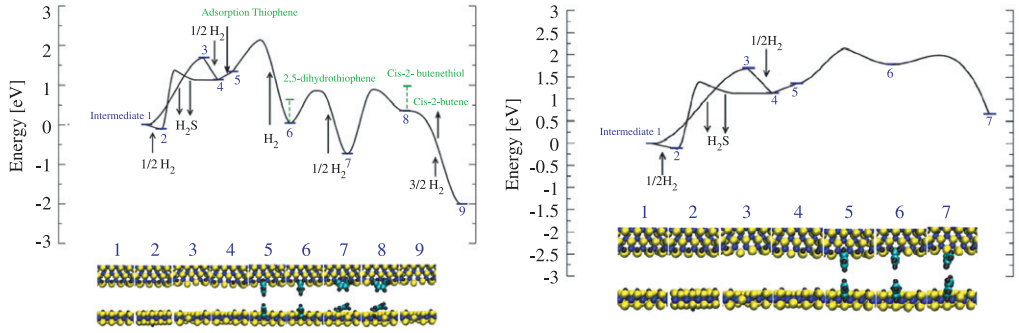

Figure 4. The hydrogenation (HYD) pathway (left) and the direct desulfurization (DDS) pathway (right) at the S edge. Colour code: molybdenum, blue; sulfur, yellow; carbon, turquoise; hydrogen, black (colours only available in the web version). Adapted from [76].

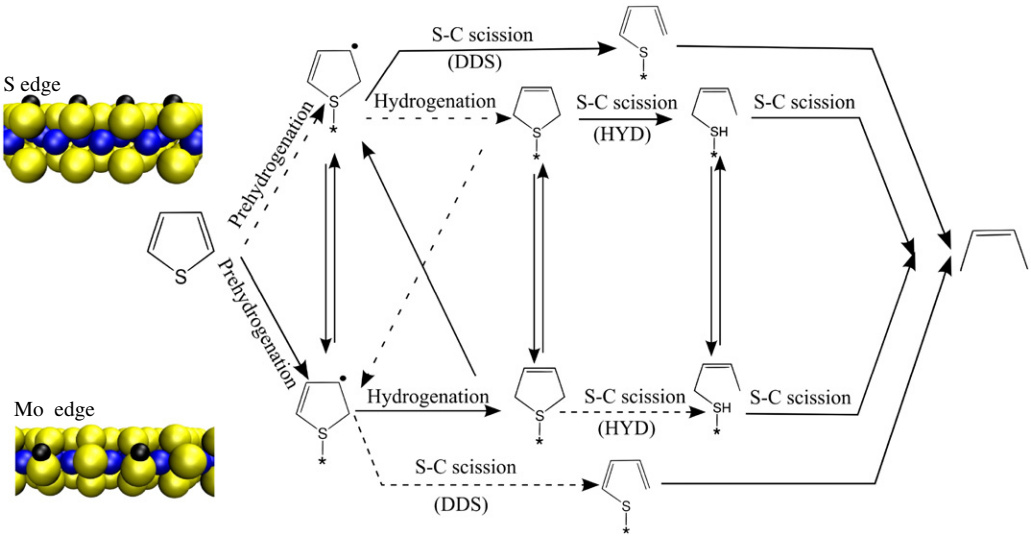

Figure 5. Schematic overview of HDS of thiophene. Upper part: the equilibrium structure at HDS conditions at the S edge and the possible reactions occurring at the S edge. Lower part: the equilibrium structure at HDS conditions at the Mo edge and the possible reactions occurring at the Mo edge. The dotted lines represent slow reactions (colour code is the same as figure 4). Adapted from [76].

unpromoted MoS_2 catalysts, and that promotion by Co and Ni introduces significant changes, as they alter both availability and structure of both edges.

The calculations provided a detailed picture of the reaction network of thiophene HDS on MoS_2, which we summarize in the schematic overview in figure 5. One important result is that the HDS reaction uses different active sites depending on the specific reaction conditions, and that the reaction is a complex interplay between Mo-edge brim sites and S-edge vacancy sites.

Another most important aspect regarding the reactivity of HDS catalyst is the mechanism of inhibition. Today, this is an increasingly important issue for catalyst manufacturers, since heterocyclic compounds inhibit the HYD pathway, which is the primary pathway for desulfurization of the most refractory species like 4,6-dimethyldibenzothiophene, which must be removed in order to fulfil present environmental regulations. The inhibition strength of nitrogen-containing heterocyclic compounds on the HYD pathway has been shown experimentally to follow the proton affinity of the nitrogen-containing compounds [100]. It has also been the subject of theoretical studies [63, 64, 70].

In a recent DFT investigation of inhibition by pyridine [70], we found that pyridine reacts with a proton at the Mo edge and forms a pyridinium ion, which binds much more strongly than pyridine itself. An electron density difference plot of the pyridinium–MoS_2 system (figure 6) shows that the pyridinium ion actually forms a chemical bond to the Mo edge. In contrast, pyridine itself and benzene only physisorb and bind weakly. This provides an explanation as to why basic compounds like pyridine can inhibit hydrogenation, whereas benzene is only a weak inhibitor. Furthermore, the formation of pyridinium ions was found only to be possible at the Mo edge, which interestingly is the edge which was identified as the primary location for hydrogenation of thiophene. This provides further evidence for the Mo edge as being the primary hydrogenation active site.

5. Conclusions and outlook

We have given an overview of our recent DFT studies of hydrodesulfurization catalysts with the aim to understand both active site structure and catalytic activity. These studies

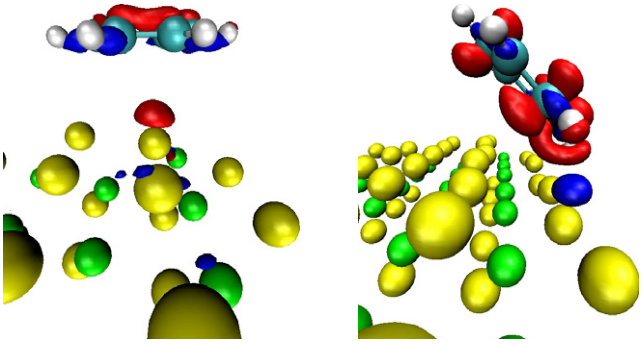

Figure 6. Electron density difference plot of benzene (left) and pyridinium (right) on the Mo edge. Note that in the pyridinium (right) plot, a proton has been transferred from the Mo edge to the pyridine molecule to form a pyridinium ion. For benzene, the depletion of electron density (red) is plotted at a contour value of -0.003 eV Å^{-3} and increase of electron density (blue) plotted at a contour value of $+0.003$ eV Å^{-3}. For pyridinium, the contour values are $+0.03$ eV Å^{-3} for electron density depletion (red) and -0.03 eV Å^{-3} for electron density increase (blue). Colour code of the atoms: sulfur, yellow; molybdenum, green; nitrogen, black; carbon, blue; hydrogen, white (colours only available in the web version). Adapted from [70].

have given us insight as to which edge structures are present under different conditions, and which sites are active for hydrogenation or sulfur extrusion reactions. For instance, by establishing the active sites for hydrogenation, one obtains information on which sites should preferentially be present in a catalyst with a high hydrogenation activity. These fundamental insights provide a basis for rational improvement of HDS catalysts.

References

[1] Topsøe H, Clausen B S and Massoth F E 1996 *Hydrotreating Catalysis—Science and Technology* vol 11, ed J R Anderson and M Boudart (Berlin: Springer)
[2] Landau M V 1997 *Catal. Today* **36** 393
[3] Gates B C and Topsøe H 1997 *Polyhedron* **16** 3213
[4] Whitehurst D D, Isoda T and Mochida I 1998 *Adv. Catal.* **42** 345
[5] Knudsen K G, Cooper B C and Topsøe H 1999 *Appl. Catal.* A **189** 205
[6] Kabe T, Ishihara A and Qian W 1999 *Hydrodesulfurization and Hydrogenation, Chemistry and Engineering* (Kodanska: Wiley–CH)
[7] Venner S F 2000 *Hydrocarb. Process.* **79** 51
[8] Song C 2003 *Catal. Today* **86** 211
[9] Babich I V and Moulijn J A 2003 *Fuel* **82** 607
[10] Topsøe H, Clausen B S, Candia R, Wivel C and Mørup S 1981 *J. Catal.* **68** 433
[11] Wivel C, Candia R, Clausen B S, Mørup S and Topsøe H 1981 *J. Catal.* **68** 453
[12] Clausen B S, Topsøe H, Candia R, Villadsen J, Lengeler B, Als-Nielsen J and Christensen F 1981 *J. Phys. Chem.* **85** 3868
[13] Topsøe N Y and Topsøe H 1983 *J. Catal.* **84** 386
[14] Breysse M, Bennett B A, Chadwick D and Vrinat M 1981 *Bull. Soc. Chim. Belg.* **90** 1271
[15] Helveg S, Lauritsen J V, Lægsgaard E, Stensgaard I, Nørskov J K, Clausen B S, Topsøe H and Besenbacher F 2000 *Phys. Rev. Lett.* **84** 951
[16] Lauritsen J V, Helveg S, Lægsgaard E, Stensgaard I, Clausen B S, Topsøe H and Besenbacher F 2001 *J. Catal.* **197** 1
[17] Lauritsen J V, Kibsgaard J, Olesen G H, Moses P G, Hinnemann B, Helveg S, Nørskov J K, Clausen B S, Topsøe H, Lægsgaard E and Besenbacher F 2007 *J. Catal.* **249** 220
[18] Carlsson A, Brorson M and Topsøe H 2004 *J. Catal.* **227** 530
[19] Carlsson A, Brorson M and Topsøe H 2006 *J. Microsc.* **233** 179
[20] Brorson M, Carlsson A and Topsøe H 2007 *Catal. Today* **123** 31
[21] Hohenberg P and Kohn W 1964 *Phys. Rev.* B **136** 864
[22] Kohn W and Sham L J 1965 *Phys. Rev.* A **140** 1133
[23] Kresse G and Furthmüller J 1996 *Comput. Mater. Sci.* **6** 15
[24] http://cms.mpi.univie.ac.at/vasp
[25] Payne M C, Teter M P, Allan D C, Arias T A and Joannopoulos J D 1992 *Rev. Mod. Phys.* **64** 1045
[26] CASTEP and DMol^3 are commercialized within the materials studio software package by Accelrys http://www.accelrys.com
[27] Delley B 2000 *J. Chem. Phys.* **113** 7756
[28] Hammer B, Hansen L B and Nørskov J K 1999 *Phys. Rev.* B **59** 7413
[29] The Dacapo code is available under the GNU general public license at http://www.camp.dtu.dk/software.aspx
[30] Gonze X, Beuken, Caracas R, Detraux F, Fuchs M, Rignanese G-M, Sindic L, Verstraete M, Zerah G, Jollet F, Torrent M, Roy A, Mikami M, Ghosez Ph, Raty J-Y and Allan D C 2002 *Comput. Mater. Sci.* **25** 478
[31] The Abinit code is available under the GNU general public license at http://www.abinit.org
[32] Schwarz K and Blaha P 2003 *Comput. Mater. Sci.* **28** 259
[33] http://www.wien2k.at
[34] Nørskov J K, Scheffler M and Toulhoat H 2006 *MRS Bull.* **31** 673
[35] Byskov L S, Hammer B, Nørskov J K, Clausen B S and Topsøe H 1997 *Catal. Lett.* **47** 177
[36] Raybaud P, Hafner J, Kresse G and Toulhoat H 1998 *Phys. Rev. Lett.* **80** 1481
[37] Raybaud P, Hafner J, Kresse G and Toulhoat H 1998 *Surf. Sci.* **407** 237
[38] Faye P, Payen E and Bougeard D 1999 *J. Mol. Modell.* **5** 63
[39] Toulhoat H, Raybaud P, Kasztelan S, Kresse G and Hafner J 1999 *Catal. Today* **50** 629
[40] Byskov L S, Nørskov J K, Clausen B S and Topsøe H 1999 *J. Catal.* **187** 109
[41] Cristol S, Paul J-F, Payen E, Bougeard D, Hafner J and Hutschka F 1999 *Stud. Surf. Sci. Catal.* **127** 327
[42] Byskov L S, Nørskov J K, Clausen B S and Topsøe H 2000 *Catal. Lett.* **64** 95
[43] Raybaud P, Hafner J, Kresse G, Kasztelan S and Toulhoat H 2000 *J. Catal.* **189** 129
[44] Raybaud P, Hafner J, Kresse G, Kasztelan S and Toulhoat H 2000 *J. Catal.* **190** 128
[45] Alexiev V, Prins R and Weber Th 2000 *Phys. Chem. Chem. Phys.* **2** 1815
[46] Ma X and Schobert H H 2000 *J. Mol. Catal.* A **160** 409
[47] Cristol S, Paul J-F, Payen E, Bougeard D, Clémendot S and Hutschka F 2000 *J. Phys. Chem.* B **104** 11220
[48] Alexiev V, Prins R and Weber Th 2001 *Phys. Chem. Chem. Phys.* **3** 5326
[49] Bollinger M V, Lauritsen J V, Jacobsen K W, Nørskov J K, Helveg S and Besenbacher F 2001 *Phys. Rev. Lett.* **87** 196803
[50] Schweiger H, Raybaud P, Kresse G and Toulhoat H 2002 *J. Catal.* **207** 76
[51] Schweiger H, Raybaud P and Toulhoat H 2002 *J. Catal.* **212** 33

[52] Travert A, Nakamura H, van Santen R A, Cristol S and Payen J F E 2002 *J. Am. Chem. Soc.* **124** 7084
[53] Cristol S, Paul J-F, Payen E, Bougeard D, Clémendot S and Hutschka F 2002 *J. Phys. Chem.* B **106** 5659
[54] Orita H, Uchida K and Itoh N 2003 *J. Mol. Catal.* A **193** 197
[55] Yang H, Fairbridge C and Ring Z 2003 *Energy Fuels* **17** 387
[56] Paul J F and Payen E 2003 *J. Phys. Chem.* B **107** 4057
[57] Bollinger M V, Jacobsen K W and Nørskov J K 2003 *Phys. Rev.* B **67** 085410
[58] Todorova T, Alexiev V, Prins R and Weber T 2004 *Phys. Chem. Chem. Phys.* **6** 3023
[59] Cristol S, Paul J-F, Payen E, Bougeard D, Hutschka F and Clémendot S 2004 *J. Catal.* **224** 138
[60] Sun M, Nelson A E and Adjaye J 2004 *J. Catal.* **226** 32
[61] Sun M, Nelson A E and Adjaye J 2005 *J. Catal.* **233** 411
[62] Sun M, Nelson A E and Adjaye J 2005 *Catal. Today* **105** 36
[63] Sun M, Nelson A E and Adjaye J 2005 *J. Catal.* **231** 223
[64] Sun M, Nelson A E and Adjaye J 2005 *Catal. Today* **109** 49
[65] Todorova T, Prins R and Weber T 2005 *J. Catal.* **236** 190
[66] Arrouvel C, Breysse M, Toulhoat H and Raybaud P 2005 *J. Catal.* **232** 161
[67] Zeng T, Wen X-D, Li Y-W and Jiao H 2005 *J. Mol. Catal.* A **241** 219
[68] Zeng T, Wen X-D, Wu G-S, Li Y-W and Jiao H 2005 *J. Phys. Chem.* B **109** 2846
[69] Zeng T, Wen X-D, Li Y-W and Jiao H 2005 *J. Phys. Chem.* B **109** 13704
[70] Logadóttir Á, Moses P G, Hinnemann B, Topsøe N-Y, Knudsen K G, Topsøe H and Norskov J K 2006 *Catal. Today* **111** 44
[71] Travert A, Dujardin C, Maugé F, Veilly E, Cristol S, Paul J-F and Payen E 2006 *J. Phys. Chem.* B **110** 1261
[72] Sun M, Nelson A E and Adjaye J 2006 *Catal. Lett.* **109** 133
[73] Wen X-D, Li Y-W, Wang J and Jiao H 2006 *J. Phys. Chem.* B **110** 21060
[74] Cristol S, Paul J F, Schovsbo C, Veilly E and Payen E 2006 *J. Catal.* **239** 145
[75] Raybaud P 2007 *Appl. Catal.* A **322** 76
[76] Moses P G, Hinnemann B, Topsøe H and Nørskov J K 2007 *J. Catal.* **248** 188
[77] Wen X-D, Ren J, Li Y-W, Wang J and Jiao H 2007 *Chem. Phys. Lett.* **436** 209
[78] Costa D, Arrouvel C, Breysse M, Toulhoat H and Raybaud P 2007 *J. Catal.* **246** 325
[79] Todorova T, Prins R and Weber T 2007 *J. Catal.* **246** 109
[80] Aray Y, Rodríguez J, Vidal A B and Coll S 2007 *J. Mol. Catal.* A **271** 105
[81] Vanderbilt D 1990 *Phys. Rev.* B **41** 7892
[82] Perdew J P, Chevary J A, Vosko S H, Jackson K A, Pederson M R, Singh D J and Fiolhais C 1992 *Phys. Rev.* B **46** 6671
[83] Tersoff J and Hamann D R 1983 *Phys. Rev. Lett.* **50** 1998
[84] Jonsson H, Mills G and Jacobsen K W 1997 Nudged elastic band method for finding minimum energy paths of transitions *Classical and Quantum Dynamics in Condensed Phase Systems: Enrico Fermi Summer School 1997* (Singapore: World Scientific)
[85] Reuter K and Scheffler M 2002 *Phys. Rev.* B **65** 035406
[86] Kam K K and Parkinson B A 1982 *J. Phys. Chem.* **86** 463
[87] Lauritsen J V, Bollinger M V, Lægsgaard E, Jacobsen K W, Nørskov J K, Clausen B S, Topsøe H and Besenbacher F 2004 *J. Catal.* **221** 510
[88] Lauritsen J V, Nyberg M, Vang R T, Bollinger M V, Clausen B S, Topsøe H, Jacobsen K W, Lægsgaard E, Nørskov J K and Besenbacher F 2003 *Nanotechnology* **14** 385
[89] Lauritsen J V, Nyberg M, Nørskov J K, Clausen B S, Topsøe H, Lægsgaard E and Besenbacher F 2004 *J. Catal.* **224** 94
[90] Wolverton C and Hass K C 2001 *Phys. Rev.* B **63** 024102
[91] Paglia G, Buckley C E, Rohl A L, Hunter B A, Hart R D, Hanna J V and Byrne L T 2003 *Phys. Rev.* B **68** 144110
[92] Paglia G, Rohl A L, Buckley C E and Gale J D 2005 *Phys. Rev.* B **71** 224115
[93] Krokidis X, Raybaud P, Gobichon A E, Rebours B, Euzen P and Toulhoat H 2001 *J. Phys. Chem.* B **105** 5121
[94] Digne M, Sautet P, Raybaud P, Euzen P and Toulhoat H 2004 *J. Catal.* **226** 54
[95] Sun M Y, Nelson A E and Adjaye J 2006 *J. Phys. Chem.* B **110** 2310
Paglia G, Buckley C E and Rohl A L 2006 *J. Phys. Chem.* B **110** 2072 1 (comment)
Digne M, Raybaud P, Sautet P, Rebours B and Toulhoat H 2006 *J. Phys. Chem.* B **110** 20719 (comment)
Nelson A E, Sun M Y and Adjaye J 2006 *J. Phys. Chem.* B **110** 20724 (reply)
[96] Hinnemann B, Nørskov J K and Topsøe H 2005 *J. Phys. Chem.* B **109** 2245
[97] Cooper B H and Knudsen K G 2006 Ultra deep desulfurization of diesel: how an understanding of the underlying kinetics can redure investment costs *Practical Advances in Petroleum Processing* ed C S Hsu and P R Robinson (New York: Springer) chapter 10, pp 297–316
[98] Egorova M and Prins R 2006 *J. Catal.* **241** 162
[99] Honkala K, Hellman A, Remediakis I N, Logadóttir Á, Carlsson A, Dahl S, Christensen C H and Nørskov J K 2005 *Science* **307** 555
[100] LaVopa V and Satterfield C N 1988 *J. Catal.* **110** 375